

2. PREPARATION OF THE SAMPLES

Silica aerogels were prepared from solutions of tetramethoxy-silane (TMOS (Fluka) dissolved in methanol. The composition varied between 20, 30, 40, 50, 60, 70 and 100 vol % of TMOS. To this solution 4 moles of bidistilled H_2O was added to each mole of TMOS. Sols have been also catalysed by adding to the water HNO_3 (pH = 2) or NH_4OH (pH = 9) in order to prepare gels under acidic, neutral and basic conditions. After 20 minutes of vigorous stirring the solutions were transferred to Pyrex tubes and hermetically closed and let to gel at 55°C. The preparation of 100 vol % TMOS leading after gelation to sonogel has been described elsewhere⁵⁻⁶.

The tubes were then opened and placed in an autoclave for drying by hypercritical solvent evacuation⁷⁻⁸; the critical conditions, $P_c = 200$ bars and $T_c = 300^\circ C$, were reached by the addition of methanol in the autoclave. The samples used for SAXS studies have been cut into thin slices using a diamond saw. Their thickness was adjusted for optimal X-ray transmission (~1 mm). The samples have been prepared in two laboratories: series I at Montpellier (acid gels) and series II in São Carlos (acid, neutral and basic gels).

3. EXPERIMENTAL

The SAXS experiments were carried at room temperature at the LURE Synchrotron radiation facility using the DC-1 position storage ring which provides an intense monochromatic beam of point like cross section at $\lambda = 1.55$ Å. This geometry eliminates the troublesome necessity of data desmearing for slit height effects and allows to obtain more precise results for testing any fractal behavior. The scattered X-rays were detected by a 1-d position sensitive detector; the data taken with an acquisition time of the order of 1 minute were stored and computer processed for background corrections and plots.

All samples used in the SAXS measurements have also been studied by N_2 BET in order to determine their specific surface $S(m^2/g)$ and their apparent density ρ_a have been determined by Hg volumetry. Transmission Electron Microscopy (TEM) microphotographs have been recorded for some samples.

4. SAXS METHOD

The intensity of X-rays scattered at low angle by a system of identical particles is:

$$I(Q) = N(\Delta\rho)^2 v^2 \exp\left(-\frac{1}{3} R_G^2 Q^2\right) \quad (1)$$

where $I(Q)$ is the SAXS intensity as a function of the modulus of the scattering vector $Q = 4\pi(\sin\theta)/\lambda$, 2θ being the scattering angle, λ the X-ray wavelength, N the number of particles of volume v and electronic radius of gyration R_G , $\Delta\rho$ the difference of electronic densities of the scattering particles and of the background.

For a polydispersed system R_G is heavily weighted towards larger particles. (R_G) can be obtained from SAXS measurements on a relative scale from a $\log I(Q)$ vs Q^2 plot. For a dense system of particles or voids (R_G) is a rough value of the correlation length. The intensity scattered at higher angles can be analysed in terms of a power law using $\log I(Q)$ vs $\log(Q)$ plots.

$$I(q) \sim A Q^{-p} \quad (2)$$

$|P|$ can be related to fractal characteristics of the particles⁹:

• For mass fractals of dimension $1 < D < 3$: $|P| = D$.

• For surface fractals of dimension $2 < D_S < 3$: $|P| = 6 - D_S$.

A particle having a smooth non fractal surface is characterized by $D_S = 2$ and $|P| = 4$, corresponding to the classic POROD's behavior. The POROD's law may therefore be generalized

$$\lim_{Q \rightarrow \infty} [I(Q) \cdot Q^p] = \text{cte} \quad (3)$$

5. MODEL

The results are analysed in term of a two density system having a volume fraction ϕ and $1-\phi$ and apparent density ρ_a . The main problem is the assignment of the respective densities of the two co-existing phases:

a) The solid "particles" of the system form the fraction ϕ of density $\rho' = \rho_g/\phi$, the remaining fraction $1-\phi$ corresponding to the air filled pores of zero density.

b) The "particles" detected by scattering effects are pores occupying a fraction ϕ , the remaining fraction $1-\phi$ corresponding to a solid matrix of density $\rho = \rho_g/(1-\phi)$. The aerogel texture can be visualised as a sponge formed by a light SiO_2 matrix containing essentially closed micropores in the 5 - 10 Å range reducing its apparent skeletal density to ρ and meso and macropores of mean

radius (R_g).

6. EXPERIMENTAL RESULTS AND DISCUSSION

6.1. Aerogels Prepared From Acidic Sols

Figure 1 is an example of the experimental SAXS curves for aerogels (series I) prepared from acidic sols with various concentrations.

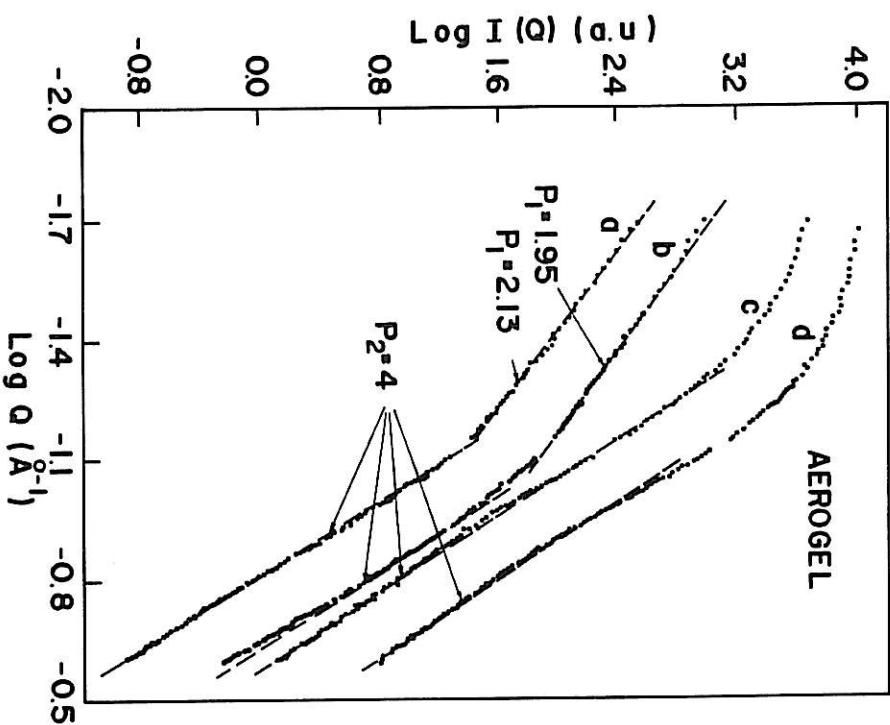


FIGURE 1

SAXS results plotted as $\log I$ vs $\log Q$ for aerogels (series I) prepared from acidic sols with the following TMOS concentration (vol %) - a) 30 b) 50 c) 70 d) 100. The curves are shifted vertically.

For low concentrations ($C < 50$ vol %) two linear regions are observed and can be analysed in term of the power law (2) with $P = 2.13 \pm 0.1$ at low Q and 4 at high Q values. These aerogels are thought to be mass fractal with dimensionality $D = 2.13$ build up by smooth (non fractal) structural units of average radius $r \sim 12R$.

SAXS results of series II show a similar behavior (low TMOS content) and Porod's law seems to be obeyed at high Q . The dimensionality D and the average radius r of non fractal structural units are given in Table 1 together with other structural parameters obtained by a method described in (10).

TABLE 1

Parameters obtained for aerogels of series I and II prepared from acidic sols.

Series	TMOS vol %	D	r [Å]	S [m ² /g]	ρ_a [g/cm ³]	ϕ (%)	ρ [g/cm ³]	ρ' [g/cm ³]	R_g^0 [Å]
I	30	2.13	-12	419	0.21	10	0.23	2.1	70
I	50	1.95	-12	421	0.39	15	0.46	2.6	65
I	70	-	-	187	0.52	16	0.62	3.3	52
I	100	-	-	288	0.69	18	0.95	2.5	39
II	30	2.23	7	782	0.21	9	0.24	2.4	159
II	40	2.28	8	859	0.35	16	0.42	2.2	100
II	50	2.17	7	862	0.43	20	0.53	2.4	81

The values of r are smaller than those of series I and the fractal dimensionality slightly higher. We believe that the texture of these aerogels is better described by a porous material of a light SiO_2 matrix (model b) since the values of ρ' are unrealistic. The matrix density ρ , the porous volume fraction ϕ and the apparent density ρ_a increase monotonically with TMOS concentration while (R_g) decreases. The difference in the absolute values of the BET areas of the two series are unexplained but appear constant at low concentration and then diminishes¹⁰.

Figure 2 shows a transmission electron microscopy of an aerogel prepared from acidic sols. This picture and previous results of Mulder et al¹¹ confirm directly that aerogels are porous materials having a matrix which occupy a higher volume fraction than voids.

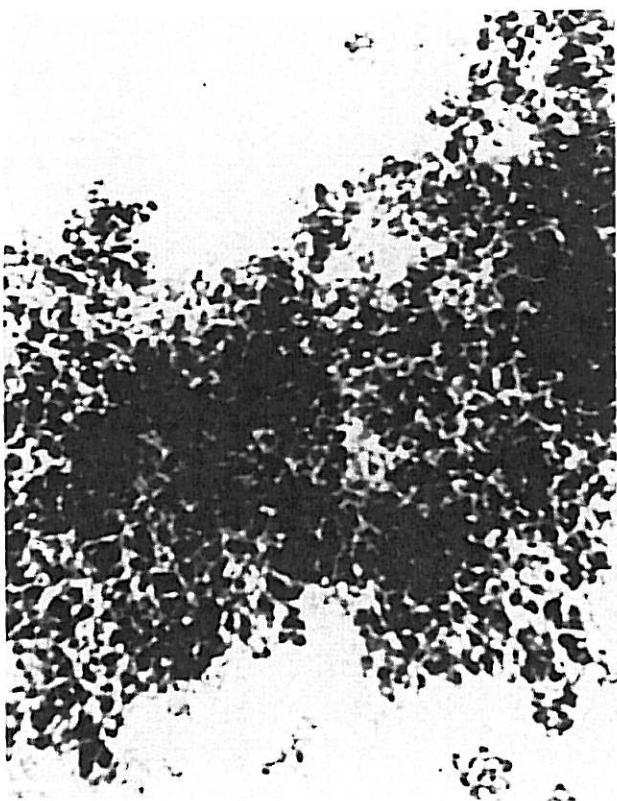


FIGURE 2
TEM microphotography of aerogel prepared from acidic sol.

6.2. Aerogels Prepared From Neutral And Basic Sols

The SAXS behavior of aerogels prepared from neutral and basic sols with TMOS concentration $C < 60\%$ is similar to the one of acidic gels, i.e, the curves $\log I(Q)$ vs $\log Q$ show two linear regions with a slope -4 at high Q and $P_1 < 3$ at low Q values. Tables 2 and 3 give all the structural parameters corresponding to series II.

The values of the matrix density ρ' corresponding to a dense matrix appear again unreal and we think that the texture of a light matrix is better applicable (model b). The aerogels are mass fractals for low length scale but with higher dimensionalities than the acidic gels. The values of D decrease with TMOS concentration. The general tendencies of the parameters ρ_a , r , R_g and ϕ for the various TMOS concentrations are close to the ones observed in acidic gels. The BET specific area remains approximately constant for each type of aerogel.

TABLE 2
Measured and calculated parameters for aerogels of serie II prepared from neutral sols.

Series	TMOS vol %	D	r [Å]	S [m ² /g]	ρ_a [g/cm ³]	ϕ (%)	ρ [g/cm ³]	ρ' [g/cm ³]	R_g [Å]
II	20	2.70	6	672	0.10	4	0.10	2.7	195
II	30	2.43	8	695	0.15	6	0.16	2.7	180
II	40	2.25	8	734	0.23	10	0.25	2.5	147
II	50	2.29	8	848	0.28	13	0.32	2.5	118
II	60	2.23	9	748	0.32	15	0.38	2.2	96

TABLE 3
Measured and calculated parameters for aerogels of serie II prepared from basic sols.

Series	TMOS vol %	D	r [Å]	S [m ² /g]	ρ_a [g/cm ³]	ϕ (%)	ρ [g/cm ³]	ρ' [g/cm ³]	R_g [Å]
II	30	2.67	12	479	0.14	6	0.14	2.4	114
II	40	2.42	14	425	0.17	7	0.18	2.6	96
II	50	2.39	14	465	0.20	8	0.22	2.4	90

7. CONCLUSIONS

The variation of the different structural parameters with concentration suggests that the number of polymeric precursor particles is larger in the more concentrated sols, giving after gelation a texture the finer as the concentration is larger. This may also be responsible for the significant decrease in fractal dimensionality for increasing TMOS concentration.

The differences observed in the parameters concerning the acid, neutral and basic gels (Tables 1, 2 and 3) suggest clear differences in their structure. The apparent aerogel density, matrix density, voids volume fraction and BET surface area, averaged for TMOS contents of 30, 40 and 50 %, are the highest for acid-catalysed gels, the lowest for the base-catalysed ones and intermediate for neutral gels.

The average radius of the structural units which build up the fractal structure or the samples of series II are in the sequence

Facid $< \tau$ neutral $< \tau$ basic. This is coherent with what is expected from the sequence of BET surface areas: S acid $> S$ neutral $> S$ basic.

The main fractal features of the aerogels are similar to the ones corresponding to the secondary structure¹ of the precursor humid gels. The only apparent structural difference between humid and dry gels concerns the structural units, which are smooth (non fractal) in aerogels and fractals in humid gels¹.

REFERENCES

- 1) T. Lours, J. Zarzycki, A.F. Craievich, D.I. dos Santos and M.A. Aegerter, this volume.
- 2) A.F. Craievich, D.I. dos Santos, M.A. Aegerter, T. Lours, J. Zarzycki, Proc. Fourth International Workshop on Glasses and Glass Ceramics From Gels, Kyoto (1986), J. Non Cryst. Solids, in print.
- 3) T. Lours, J. Zarzycki, D.I. dos Santos, M.A. Aegerter and A.F. Craievich, Proc. Fourth International Workshop on Glasses and Glass Ceramics From Gels, Kyoto (1986), J. Non Cryst. Solids, in print.
- 4) E.C. Ziemath, M.A. Aegerter, J.E.C. Moreira, T. Lours and J. Zarzycki, Proc. Fourth International Workshop on Glasses and Glass Ceramics From Gels, Kyoto (1986), J. Non Cryst. Solids, in print.
- 5) L. Esquivias and J. Zarzycki, 3rd Int. Conference Ultrastructure Processing of Ceramics, Glasses and Composites, San Diego (USA), 1987.
- 6) L. Esquivias and J. Zarzycki, Proc. First Int. Workshop on Non-Crystalline Solids, San Felu de Guixols (Spain), M.D. Bard, N. Clavaguera, ed., World Scientific. (1986).
- 7) J. Zarzycki, M. Prassas and J. Phalippou, J. Mater. Sci. 17 (1982) 3371.
- 8) D.I. dos Santos, N.D.S. Mohallem, M.A. Aegerter, Cerâmica 197 (1986) 109.
- 9) D.W. Scheefer and K.D. Keefer, Phys. Rev. Lett. 53 (1984) 1383.
- 10) A.F. Craievich, M.A. Aegerter, D.I. dos Santos, T. Woignier and J. Zarzycki, J. Non Cryst. Solids 86 (1986) 394.
- 11) C.A.M. Mulder, G. Van Leuven, J.G. Van Lierop and J.P. Woerdman, J. Non Cryst. Solids, 82 (1986) 148.